Journal of Magnetic Resonance 199 (2009) 136–145

Contents lists available at ScienceDirect

Journal of Magnetic Resonance

journal homepage: www.elsevier.com/locate/jmr

Repetition time and flip angle variation in SPRITE imaging for acquisition time and SAR reduction

N. Jon Shah [a,b,*], Joachim B. Kaffanke [a], Sandro Romanzetti [a]

[a] Institute of Neuroscience and Medicine 4, Forschungszentrum Jülich GmbH, 52425 Jülich, Germany
[b] Department of Neurology, RWTH Aachen University, 52074 Aachen, Germany

ARTICLE INFO

Article history:
Received 7 October 2008
Revised 28 January 2009
Available online 4 February 2009

Keywords:
Single point imaging
SPRITE
SAR reduction
Acquisition time reduction
Sequence design

ABSTRACT

Single point imaging methods such as SPRITE are often the technique of choice for imaging fast-relaxing nuclei in solids. Single point imaging sequences based on SPRITE in their conventional form are ill-suited for *in vivo* applications since the acquisition time is long and the SAR is high. A new sequence design is presented employing variable repetition times and variable flip angles in order to improve the characteristics of SPRITE for *in vivo* applications. The achievable acquisition time savings as well as SAR reductions and/or SNR increases afforded by this approach were investigated using a resolution phantom as well as PSF simulations. Imaging results in phantoms indicate that acquisition times may be reduced by up to 70% and the SAR may be reduced by 40% without an appreciable loss of image quality.

1. Introduction

Magnetic Resonance Imaging (MRI) has demonstrated itself to be an excellent method of visualization of internal structures *in vivo*. The majority of these applications are based on proton imaging, that is, largely imaging of free water with relatively long-lived MR signals which is amenable to the traditional spin echo or gradient echo methods. There are, however, many interesting and important systems where the MR signal durations are short, <10–20 ms, and therefore not readily visualised using standard techniques. This is especially true if the goal is quantitative imaging of the so-called fast-relaxing nuclei such as sodium and oxygen.

The *in vivo* deployment of MRI methods originally conceived to image systems with short relaxation times due, for example, to surface relaxation in water-bearing porous materials or quadrupolar relaxation of quadrupolar nuclei in anisotropic environments has been attracting growing interest [1,2]. However, the *in vivo* adoption of the aforementioned methods is faced with two additional constraints: overall acquisition time is much more limited and the amount of energy that may be deposited, the specific absorption rate (SAR), is a severe restriction, especially for use in humans.

SPRITE (Single Point Ramped Imaging with T1 Enhancement) [3] is a purely phase encoding MRI technique. Low flip angle, broadband RF pulses are applied in the presence of phase encode gradients and after an encoding time, t_p, a single datum or multiple-points with a dwell time, Δt_p, are acquired with each of those points rebinned to different k-spaces [4]. SPRITE is an ideal technique for the imaging of fast-relaxing nuclei. However, in comparison to echo-based methods such as FLASH, SPRITE is time consuming and the SAR is higher. Major reductions in the acquisition times can be attained through use of the Spiral-SPRITE, Conical-SPRITE, and Sectoral-SPRITE sequences [5,6] and these have been demonstrated in a number of different situations [7–10].

Notwithstanding the success of the SPRITE variants, which have included a demonstration of ^{23}Na *in vivo* imaging in humans [10], further improvements are required to bring SPRITE methodology into the preclinical/clinical domains. Developments aimed at reducing the overall acquisition time and the SAR are therefore of the utmost importance.

SPRITE requires many more RF pulses than conventional sequences such as FLASH. This is the dominant problem for *in vivo* SPRITE imaging where the maximum SAR is limited by law. Further, in the case of non-proton imaging with nuclei such as ^{23}Na, the SNR is low and hence a large number of averages are needed. Improvement of the SNR by resorting to higher static field strengths is only a partial answer since this forces a further increase of the SAR. Thus, strategies for the reduction of SAR are desperately needed. One possible opportunity for the reduction of SAR is to implement a k-space position dependent variation of the flip angle. Since image signal intensity is largely determined by the signal intensity in the centre of k-space, the flip angle in the outer parts of k-space can be reduced to affect an overall reduction of the SAR.

* Corresponding author. Address: Institute of Neuroscience and Medicine 4, Forschungszentrum Jülich GmbH, 52425 Jülich, Germany. Fax: +49 2461 61 8294.
E-mail address: n.j.shah@fz-juelich.de (N. Jon Shah).

1090-7807/$ - see front matter © 2009 Elsevier Inc. All rights reserved.
doi:10.1016/j.jmr.2009.01.036

In general, once the RF pulse envelope has been constrained, two approaches of flip angle variation are possible. Either the pulse power or the pulse length can be modulated. The SAR is linearly dependent on pulse length but is a quadratic function of the B_1 field; the flip angle itself is linearly dependent on B_1. Therefore, variation of pulse magnitude is a more efficient means of affecting SAR reduction. A combination of both these approaches can, in principle, allow a reduction in SAR whilst keeping the flip angle constant.

Notwithstanding the major reductions in acquisition time for SPRITE-based sequences noted above, further reductions are required. These further reductions are necessary in order to broaden the applicability and appeal of the SPRITE methodology. The overall acquisition time can be reduced by reducing the repetition time, TR, of a given pulse-encode-acquire module depending on k-space position. The self-spoiling gradients are higher in the outer parts of k-space and therefore the repetition time can be shortened with only minor influences on the point spread function (PSF). Since the image signal intensity is largely determined by the signal intensity in the centre of k-space, the TR can be reduced in the periphery of k-space in order to reduce the overall acquisition time. Around the centre of k-space, where the gradients are low and the SNR is higher, longer repetition times are needed to allow for sufficient longitudinal relaxation to avoid saturation effects and the acquisition of residual magnetisation excited by the preceding RF pulses. An incidental advantage of a variable TR, over and above a reduction in acquisition time, is an improvement of data quality by allowing the use of a longer TR at the centre of k-space.

The work presented here demonstrates the implementation of a variable TR and variable flip angles into a SPRITE sequence. Simulation results, through a systematic variation of parameters, are presented to show the influence of reduced TR and flip angle variation. Imaging results from a structured resolution phantom are also presented to support the assertion that the new method is relevant for *in vivo* preclinical/clinical applications because it is capable of faster data acquisition with a reduced SAR.

2. Theory

2.1. Acquisition time reduction with variable TR

An example of a SPRITE gradient ramp with a variable TR in the first phase encode dimension is shown in Fig. 1a. A sequence timing diagram for a single phase encode step with the implementation of TR reduction in the form of a variable post-delay is shown in Fig. 1b. The TR reduction method can be applied in all three spatial dimensions with suitable functions, such as Gaussian or linear functions used to define the variation of TR. In two and three dimensions, the magnitude of the total gradient can be used as parameter for the variation function to provide radial symmetry. Following this concept, then, the adaptation to Spiral-SPRITE, Conical-SPRITE, or Sectoral-SPRITE is straightforward.

The repetition time was modulated by a Gaussian function depending on the radius in k-space. Additionally, a constant part with radius R around the origin of k-space and an overall offset was defined for the variation function:

$$\mathrm{TR}(k) = \mathrm{TR}_{\max}\begin{cases} 1 & k \leqslant R \\ (1-\mathrm{offset})e^{-\frac{(k-R)^2}{2\sigma^2}} + \mathrm{offset} & k > R \end{cases} \quad (1)$$

where $k = |\boldsymbol{k}|/|\boldsymbol{k}_{\max}|$, σ defines the width of the Gaussian function (σ^2 is the variance), offset ensures a minimum amplitude and R is the radius on which the function has maximum amplitude. Note that the choice of a Gaussian function is purely heuristic.

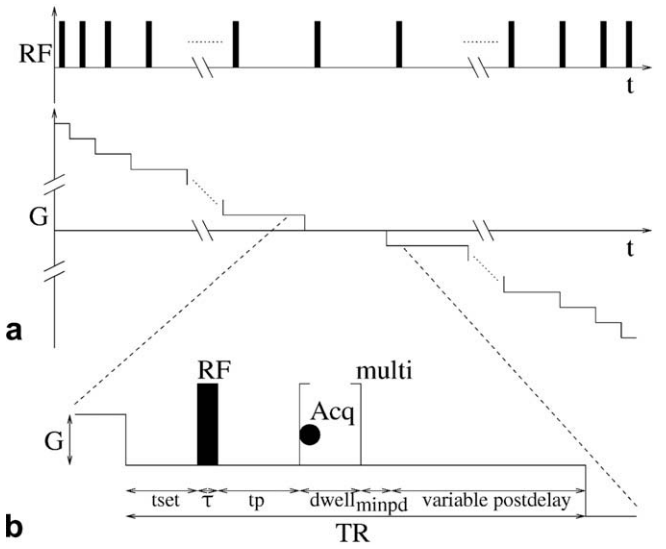

Fig. 1. (a) Schematic representation of a SPRITE gradient ramp with variable repetition time, TR. (b) Schematic representation of the m-SPRITE sequence timing diagram for a single phase encode step. The repetition time, TR, is altered here with a variable post-delay. The abbreviations used are: minpd: the minimum constant pre-delay; pw: the RF pulse length; tp: the encoding time between RF pulse and acquisition; dwell: the dwell time between the multiple acquisition points; tset: the settling down time after the gradient step, and before the next step.

2.2. SAR reduction by pulse variation

The possible approaches for pulse variation are shown in Fig. 2. The pulse amplitude or the pulse length can be modulated, independently, or a combination of these two can be utilised. The SAR for rectangular pulses is linearly dependent on the pulse length but is a quadratic function of the pulse amplitude, therefore, variation of the pulse amplitude is more efficient for SAR reduction.

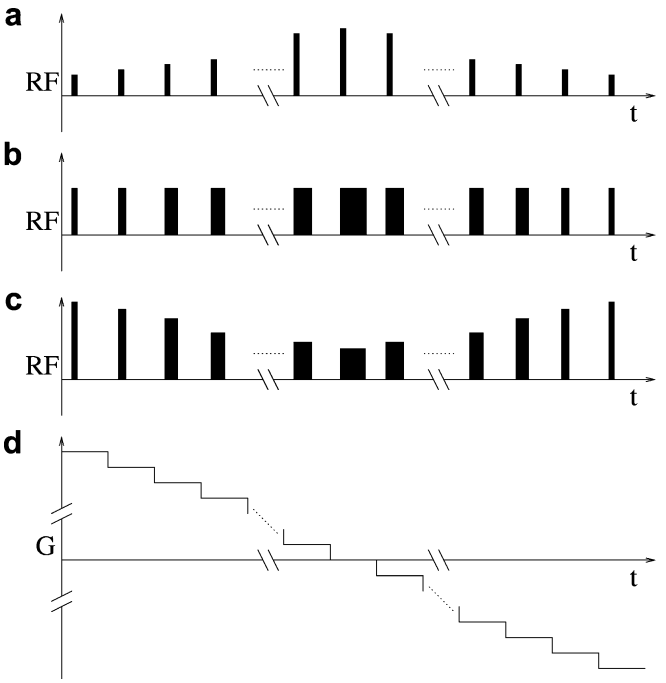

Fig. 2. (a) Schematic representation of SAR reduction with variable pulse amplitudes. (b) SAR reduction with variable pulse lengths. (c) SAR reduction using a combination of variable pulse amplitudes and pulse lengths but maintaining a constant flip angle. (d) Schematic representation of gradient ramp in SPRITE.

The combination of both methods allows the possibility of reducing the SAR whilst keeping the flip angle constant.

According to the description given by Haacke [11], SAR can be estimated as follows:

Consider the power deposition, P, in a sphere of radius R with conductivity σ', given by:

$$P = \frac{4}{15}\pi\sigma'\omega^2 B_1^2 R^5. \tag{2}$$

The applied power is quadratic in B_1. For a rectangular pulse of length τ as used in the SPRITE sequence, it follows that:

$$P = \frac{4\pi\sigma'\omega^2\alpha^2 R^5}{15\tau^2\gamma^2}: \tag{3}$$

where $\alpha = \gamma B_1 \tau$.

The resulting energy is the integral of the power deposition over time

$$W = \int_0^\tau \mathrm{P}\ \mathrm{dt} \tag{4}$$

and the SAR is proportional to the average energy deposition per repetition time:

$$\mathrm{SAR} \propto \frac{W}{\mathrm{TR}}. \tag{5}$$

Hence, the SAR is a quadratic function of B_1 and a linear function of pulse length, τ.

$$\mathrm{SAR} \propto \frac{4\pi\sigma'\omega^2 B_1^2 R^5 \tau}{15\mathrm{TR}} \tag{6}$$

This means that a decrease of pulse amplitude is the most efficient way to reduce the overall SAR (Fig. 2a). This is also preferable since the bandwidth of the pulse is kept constant. However, in the presence of small phase encode gradients the bandwidth of the pulse can be reduced [12]. Thus, the pulse length can be increased. In this case, an approach with variable pulse length can be used to increase the pulse area and, therefore, the flip angle in the centre of k-space to achieve a higher SNR (Fig. 2b). An increase of pulse length with constant flip angle may also be used for SAR reduction (Fig. 2c) without entirely sacrificing the reduction of SAR afforded by varying pulse amplitude. However, a drawback of the latter approach is the strongly varying bandwidth that leads to edge enhancement artefacts in the images.

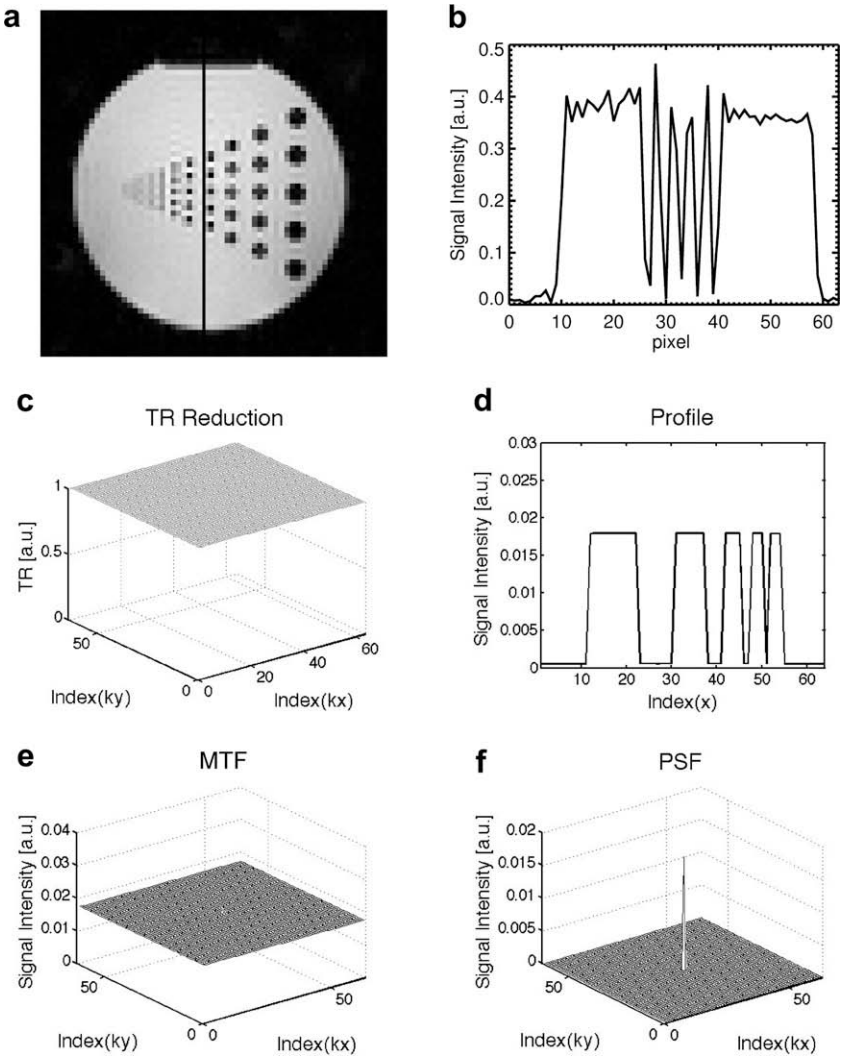

Fig. 3. A SPRITE image of a resolution phantom and a vertical profile (dark line in (a)) are shown in the top row acquired with a constant TR = 3.6 ms for a total acquisition time of 9 min 36 s. Simulation results are shown in the bottom row including MTF, PSF, a phantom profile and the reduction function. The PSF maximum contains 94% of the total distributed signal.

In the present implementation, a Gaussian function was used separately for each variable pulse amplitude (Fig. 2a) and pulse length (Fig. 2b):

$$\alpha(k) = \alpha_{\max}\begin{cases} 1 & k \leqslant R \\ (1-\text{offset})e^{-\frac{(k-R)^2}{2\sigma^2}} + \text{offset} & k > R \end{cases} \quad (7)$$

where $k = |\mathbf{k}|/|\mathbf{k}_{\max}|$, σ defines the width of the Gaussian function (σ^2 is the variance), offset ensures a minimum amplitude and R is the radius on which the function has maximum amplitude.

For the combined method (Fig. 2c), a hyperbolic function was used to define the pulse amplitude whereas the pulse length was calculated from the resulting pulse power in order to achieve a constant flip angle. Since TR reduction and SAR reduction are independent of each other, the two can be very simply combined in one pulse sequence.

3. Methods

A standard SPRITE sequence was implemented on a 4T whole-body VARIAN Unity Inova (Palo Alto, Ca., USA). The TR and flip angle reduction function was programmed in the first two phase encode dimensions such that, in k-space, a planar-based TR (and flip angle) reduction paradigm was realised. Additionally, a constant plateau around the centre and an overall offset were employed as defined in the Eqs. (1) and (7).

The effect of repetition time and flip angle variation was investigated by imaging a resolution phantom filled with transformer oil. Transformer oil was used to avoid B_1 field inhomogeneities caused by dielectric resonance effects. The FOV was set to $256 \times 256 \times 256\ \text{mm}^3$ and the matrix size was $64 \times 64 \times 32$ for all experiments.

The longitudinal relaxation time of the transformer oil phantom, T_1 = 199 ms, was measured with a standard inversion recovery pulse sequence including an additional spoiling gradient to avoid transverse magnetisation arising from imperfections of the inversion pulse. The effective transverse relaxation time was estimated from the bulk FID to be T_2^*=1.26 ms.

Point Spread Function (PSF) simulations in three dimensions were performed in Matlab 7.0 (MathWorks, Natick, Ma., USA). Both, the longitudinal and the transverse relaxation with additional spoiling by phase encoding gradients were included in the calculation of the Modulation Transfer Function (MTF). The PSF was then obtained by applying a Fourier Transform to the MTF. For demonstration purposes, the simulations were performed assuming an artificial resolution phantom.

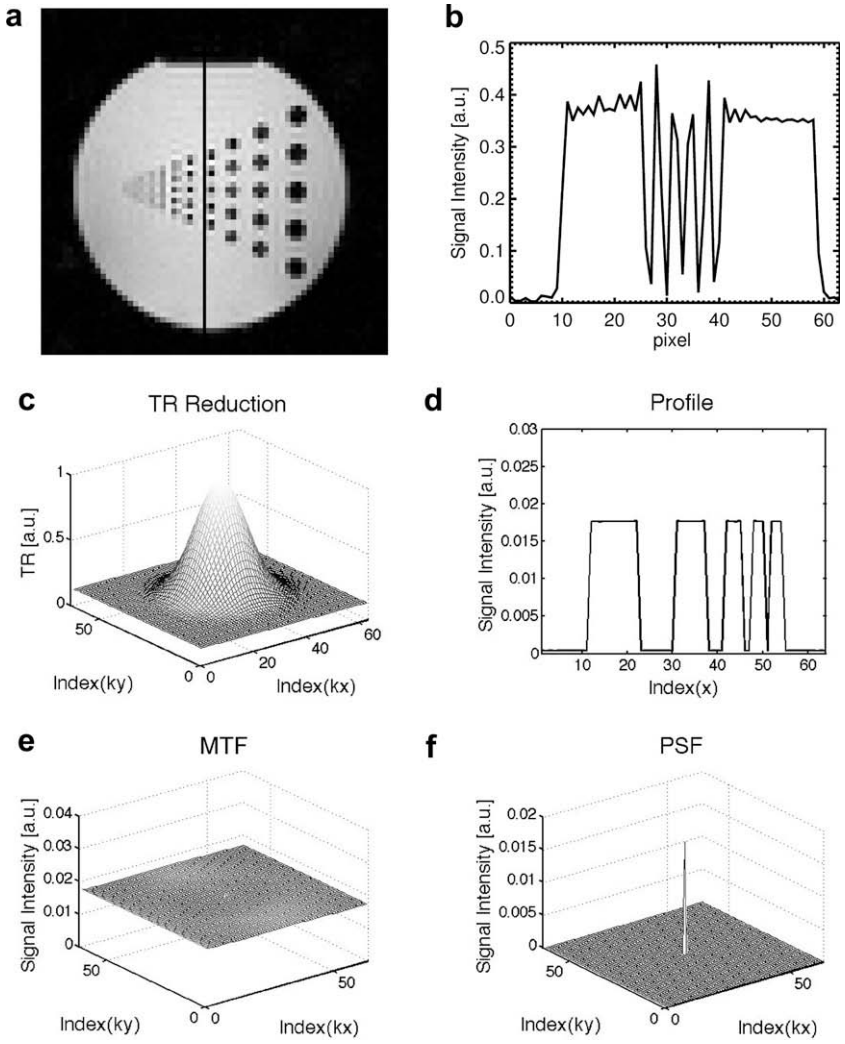

Fig. 4. A SPRITE image of a resolution phantom and a vertical profile are shown in the top row acquired with a total acquisition time of 2 min 53 s (~30% of the 'standard' acquisition time (c.f. Fig. 3)) and with TR_{max} = 3.6 ms. The same RF pulse train was used as for the experiments shown in Fig. 3. Simulation results are shown in the bottom row including MTF, PSF, a phantom profile and the reduction function. TR reduction: σ = 0.125, offset = 0.0, R = 0.0. The PSF maximum contains 90% of the total distributed signal.

The maximum repetition time (TR_{max}) for the investigation of the effect of repetition time variation was set to 3.6 ms. The encoding time was t_p = 200 μs with a dwell time of Δt_p = 6.25 μs. The settling down time after acquisition was t_{set} = 0.1 ms and a delay of 50 ms between SPRITE ramps was used. A broadband RF pulse with flip angle $\alpha = 1^\circ$ and a pulse length of 6.25 μs was used; the maximum flip angle used was 1°. Accordingly, the acquisition filter bandwidth was set to 80 kHz [12]. These parameters were also used to demonstrate an optimised experiment with the combined repetition time and flip angle variation methods. In this case, the flip angle was altered by pulse amplitude variation and a Gaussian function was used to define both TR and flip angle variations; TR_{max} was 1.2 ms and all other parameters were unchanged.

4. Results and discussion

The experimental results obtained with the non-modified sequence with a long repetition time, TR = 3.6 ms, are shown in Fig. 3(a, b). The total acquisition time was 9 min 35 s. The image does not show strong artefacts, as demonstrated by the slice profile. The related simulations show a constant MTF and a PSF maximum intensity with 94% of the total signal distributed in image space resulting in a nearly optimal simulated image profile.

The acquisition time was reduced by 70% to 2 min 53 s by TR reduction. Imaging results and a slice profile are shown in Fig. 4(a, b). The variance of the Gaussian function was set to 1/8 of the matrix size with (σ = 0.125) and the offset and the radial plateau, R, were set to zero. The quality of the profile has not been significantly degraded although the reduction in acquisition time of 70% is substantial. The simulations support this experimental observation; the MTF is nearly constant and the PSF maximum intensity has 90% of the total distributed signal.

A similar acquisition time of 2 min 42 s was achieved using a constant repetition time TR = 0.444 ms. The obtained experimental results are shown in Fig. 5(a, b). The simulation results show significant residual magnetisation around the k-space centre in the MTF. The intensity of the PSF maximum intensity has only 50% of the total signal whereas the other 50% of the signal is distributed over the rest of image space. This leads to background signal in the image and to a poor slice profile. The same effect can also be seen in the simulated profile. A comparison of Figs. 4 and 5 is very instructive at this juncture. It can be clearly seen that the TR reduction method offers the advantage of avoiding artefacts caused by residual magnetisation that mainly occur

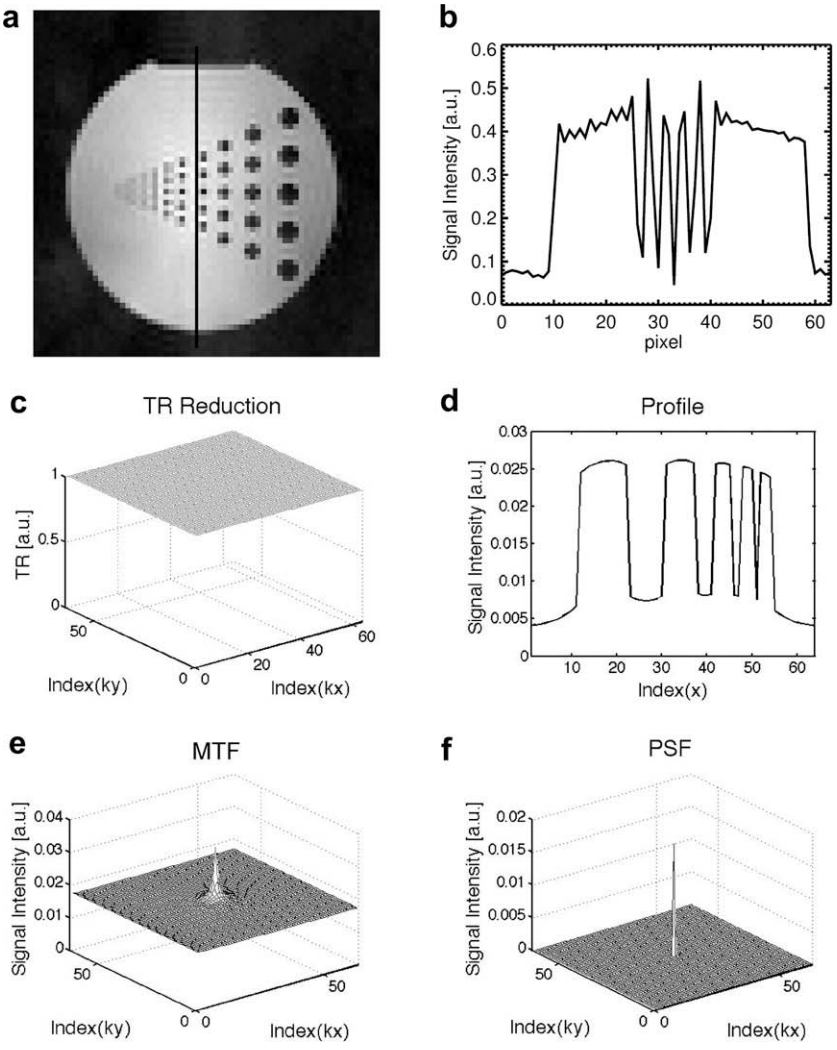

Fig. 5. A SPRITE image of a resolution phantom and a vertical profile are shown in the top row acquired with a total acquisition time of 2 min 42 s and with TR = 0.444 ms. The nominal SAR was 100%. Simulation results are shown in the bottom row including MTF, PSF, a phantom profile and the reduction function. The PSF maximum contains 50% of the total distributed signal.

around the k-space centre but nevertheless permits reasonable acquisition times.

A combination of repetition time and flip angle reduction is shown in Fig. 6(a, b). Here, TR reduction was affected in the same way as for the experiments shown in Fig. 4. Additionally, SAR reduction was realised by pulse amplitude variation. In this respect the variance of the Gaussian function was set to 1/4 of the matrix size with ($\sigma = 0.25$) and the offset and the radial plateau, R, were set to 0.5. With these parameters, images of acceptable quality were acquired. The influence of flip angle variation on the PSF shows a stronger effect than repetition time variation. This may be explained by the direct influence of the flip angle variation on the MTF and the related PSF, where only 49% of signal intensity is concentrated in the PSF maximum. A maximum SAR reduction of 40% was found to be tolerable; further reductions lead to unacceptable PSF blurring.

The experimental results of both variable pulse length and variable pulse amplitude are shown in Fig. 7 and compared with a non-reduced scan. TR reduction was used for all scans presented in this Figure. Both methods show qualitatively equivalent imaging results when used with an identical Gaussian function as can be seen by comparison of the plotted profiles. Since the SAR reduction is higher with a variable pulse amplitude, it will be the preferred method for *in vivo* applications. For studies of non-biological materials, where SAR does not play an overriding role, a variable pulse length may be used to increase the flip angle in the centre, and hence the overall image SNR, but with a concomitant increase in the SAR.

The simulation results related to Fig. 7 with variable pulse amplitude are shown in Fig. 8. An SAR reduction of 40% delivers reasonable imaging results whereas higher reductions result in a significant loss in image quality because of a poorer PSF. As such, with an SAR reduction of more than 80%, the PSF maximum reduces to 25% of the total signal available.

A combination of both, pulse amplitude and pulse length variation, presents the opportunity to reduce the SAR whilst still maintaining a constant flip angle. Imaging results using this technique are shown in Fig. 9. Under the constraint of reasonable image quality, a maximum SAR reduction of about 25% was achievable which is not as good as the 40% reduction that can be reached by variation of pulse amplitude alone. Further, the huge variation of the pulse bandwidth leads to strong edge enhancements in the images since the RF pulses applied in the outer parts of k-space have the highest

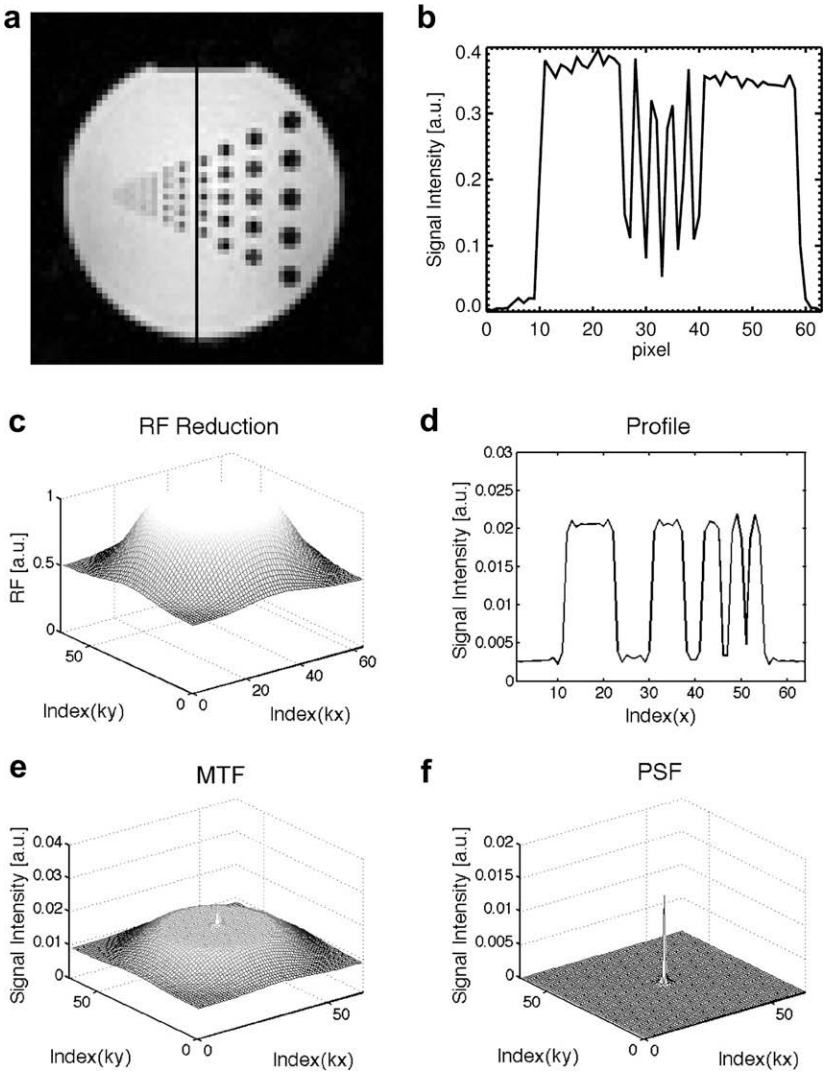

Fig. 6. A SPRITE image of a resolution phantom and a vertical profile are shown in the top row acquired with a total acquisition time of 2 min 53 s (~30% of the 'standard' acquisition time (c.f. Fig. 4)) and TR_{max} = 3.6 ms; TR reduction $\sigma = 0.125$, offset = 0.0, $R = 0.0$; flip angle reduction: $\sigma = 0.25$, offset = 0.5, $R = 0.5$, with pulse power variation. The nominal SAR was 58.4%. Simulation results are shown in the bottom row including MTF, PSF, a phantom profile and the reduction function. The PSF maximum contains 49% of the total distributed signal.

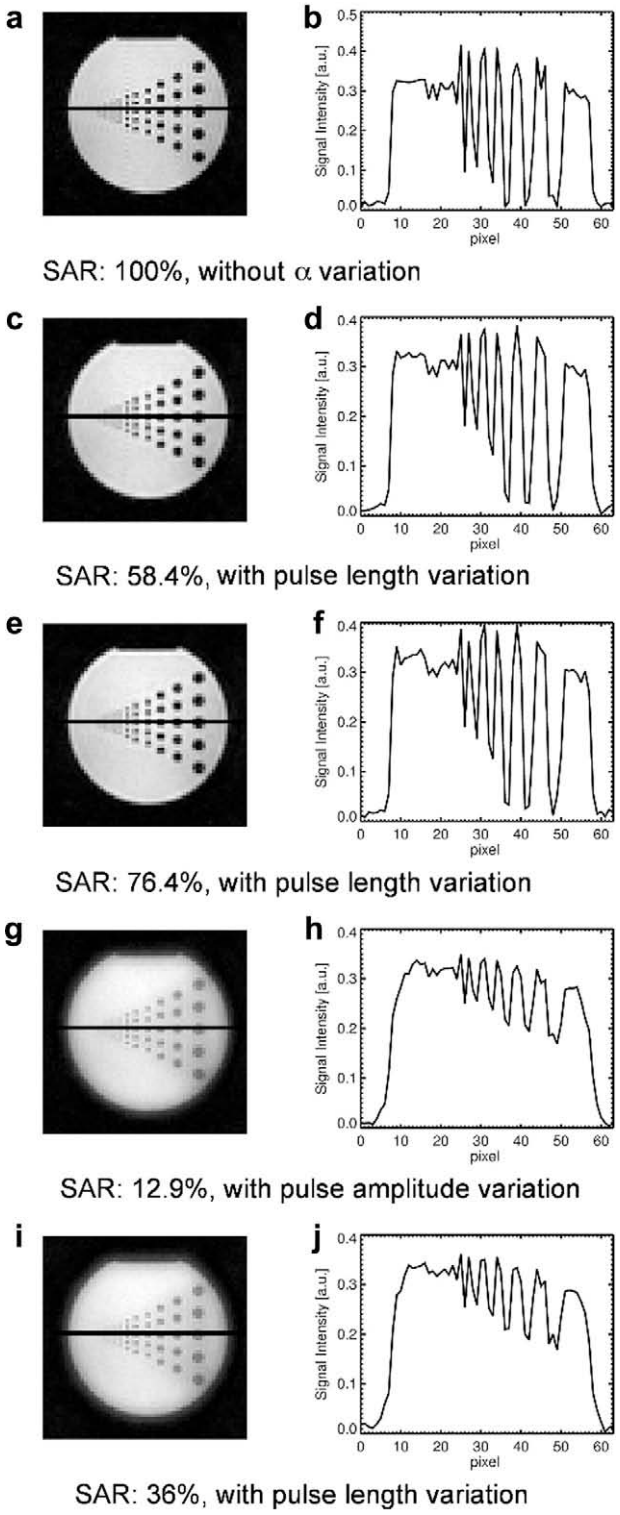

Fig. 7. Imaging results and horizontal profiles acquired with no flip angle reduction (a, b); flip angle reduction with $\sigma = 0.25$, offset = 0.5, $R = 0.5$ for variation of pulse amplitude (c, d) and pulse length (e, f); flip angle reduction with $\sigma = 0.125$, offset = 0.29, $R = 0.0$ for variation of pulse amplitude (g, h) and pulse length (i, j).

bandwidth (see Fig. 2). In general, therefore, this technique will not be the preferred method for SAR reduction.

Many groups have proposed short T_2^* imaging methods based on the acquisition of echoes. Three-dimensional projection reconstruction (PR) has been adopted by several groups [13,14]. Unfortunately, PR techniques can corrupt the origin of k-space, due to the RF probe ring down and/or gradient switching, and therefore require data correction and gridding prior to Fourier reconstruction. The PR technique is not an imaging method wherein contrast can be as easily manipulated as in SPRITE [15] and since PR imaging is based on echo encoding it has an inherent resolution limitation because of the convolution of the signal with the T_2^* decay. In

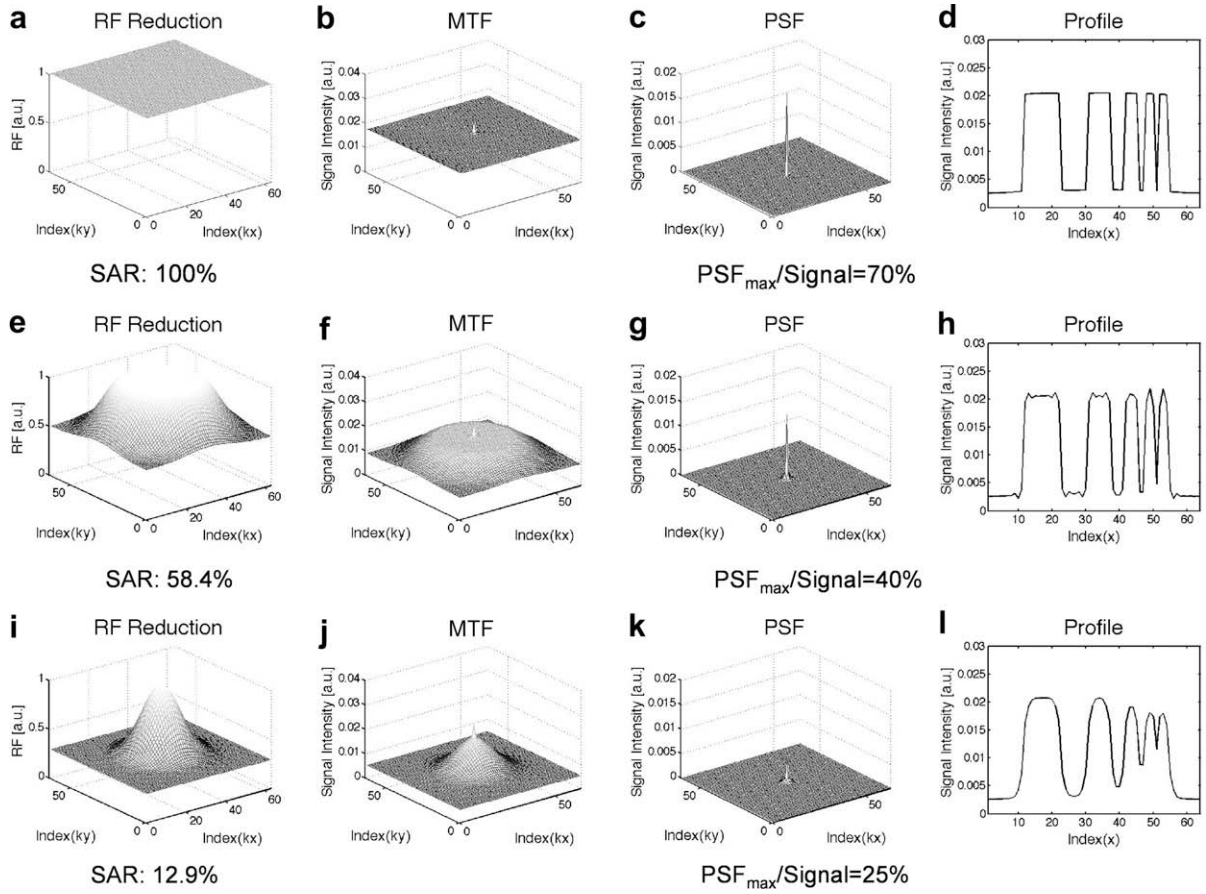

Fig. 8. Simulation results using variable pulse amplitude with the same parameters as in Fig. 7 (a, b), (c, d) and (g, h) demonstrate the strong influence of flip angle variation on the PSF (c, g, k), and the relative intensity of the PSF maximum. These were calculated from the MTF (b, f, j) using the reduction function for pulse amplitude (a, e, i), which defines the achieved SAR reduction. The simulated profiles (d, h, l) are in good agreement with the measurement results in Fig. 7 The parameters were: (a–d) no flip angle reduction; (e–h) flip angle reduction with $\sigma = 0.25$, offset = 0.5, $R = 0.5$; (i–l) flip angle reduction with $\sigma = 0.125$, offset = 0.29, $R = 0.0$.

comparison with echo-based methods such as PR and its newer variant, ultra-short TE (UTE) imaging [16], the longer acquisition times and the required large number of RF pulses are inherent disadvantages of SPI methods which include SPRITE. As a consequence, the applicability of SPRITE, in its standard form, for *in vivo* applications is severely restricted. The twin obstacles, long acquisition times and high SAR, must be overcome if the advantages of SPRITE are to be realised; these include immunity to T_2^* convolution, easily manipulated contrast, and suitability for relaxation time mapping and density mapping in particular. The work presented here demonstrated strategies for overcoming the aforementioned obstacles that stand in the way of SPRITE imaging for human applications.

Variation of repetition time influences the T_1 weighting that may be different in SPRITE with a constant TR. PSF maximum peak intensities (in percent) calculated for different combinations of TR and T_1 are given in Table 1. For the case of constant TR, the influence of T_1 may be completely neglected if $TR = T_1$ or if $TR = 10T_1$. If $TR = 0.1T_1$, then T_1 has a small influence (that is, the maximum of the PSF intensity is reduced by about 1.5% from its nominal 100%). For the case of variable TR, the influence of T_1 is much more significant. If T_1 is long (10 s) then there is a large reduction in the maximum of the PSF intensity (~19%). Considering a more realistic T_1 of 0.1 s, however, a worst case reduction in the maximum of the PSF intensity is <2% (see Table 1).

A possible variation of the T_1 weighting over k-space affects the quality of the PSF. As such, it is noted that the accuracy of density mapping using variable TR and variable flip angle SPRITE will be compromised and be more difficult. Further work is needed to clarify this issue. Compared with the alternative use of a constant, short TR, the PSF benefits from an increased TR for transverse relaxation around the centre of k-space reducing residual magnetisation that causes image artefacts. The use of a phase cycling filter, as demonstrated, for example by Kaffanke et al. [17], annihilates residual magnetisation and therefore allows for the use of minimal repetition times.

The variation of flip angles has a strong influence on the PSF and the resolution. The technique not only influences the T_1 weighting but functions as a filter suppressing the higher frequencies and therefore spatial resolution information. The technique should in general be used with care but may be necessary for *in vivo* applications on humans at high field strength of 4 Tesla and above.

5. Conclusions

Methods for the reduction of acquisition time and SAR in SPRITE-based sequences through the use of a variable TR and variable flip angles have been presented. The concepts were simulated and experiments performed to support the simulations. Good qualitative agreement has been demonstrated between experiment and simulation.

It was shown that acquisition time reductions of about 70% and SAR reduction of about 40% can be achieved with repetition time and flip angle variation, respectively. However, both methods have

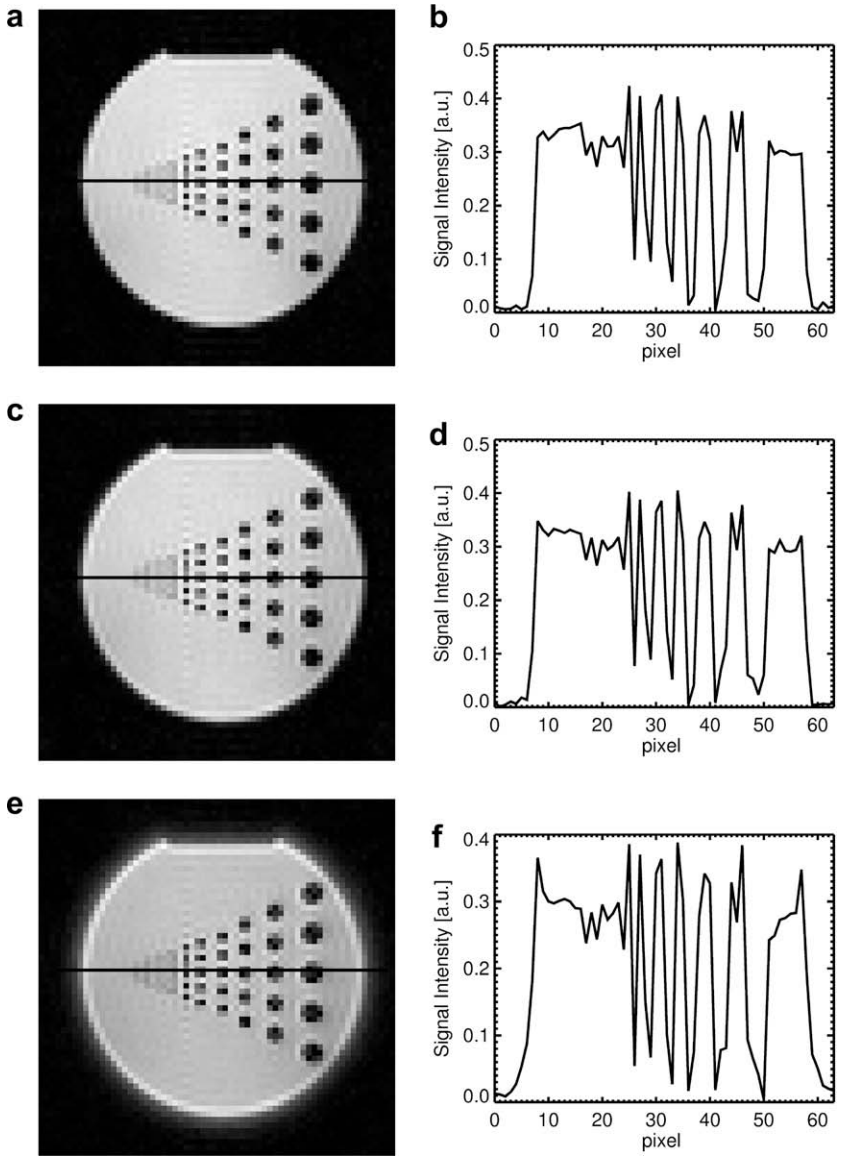

Fig. 9. SPRITE imaging results are shown acquired with combined pulse power and pulse length variation. A hyperbolic function was used for modulation with a reduction of pulse power at the centre with respect to the edges of k-space with nominal 100% pulse power. The pulse power reductions were: 20% (a, b); 50% (c, d); 80% (e, f). With the flip angle held constant, SAR reductions of 7.6% (a, b), 17.5% (c, d) and 24.4% (e, f) were achieved.

Table 1
PSF maximum peak intensities (in percent) calculated for different combinations of TR and T_1. In the case of variable TR, a minimum repetition time, TR_{min}, was utilised in each simulation. This time is the minimum time needed to: step up (or down) the gradient ramp, play out an RF pulse, wait for the selected encoding time t_p and acquire a single FID point. According to the parameters used in the experiments TR_{min} was 440 μs. The simulations also took account of the 50 ms delay between successive SPRITE ramps, which was used in real experiments to avoid excessive gradient duty cycle during the measurements.

	$TR = 0.1T_1$	$TR = T_1$	$TR = 10T_1$	
TR const	99.865	99.991	100.000	$T_1 = 0.1$ s
	99.857	99.991	100.000	$T_1 = 1$ s
	99.856	99.991	100.000	$T_1 = 10$ s
TR var	98.831	98.951	99.035	$T_1 = 0.1$ s
	91.794	92.955	93.719	$T_1 = 1$ s
	80.998	84.699	86.940	$T_1 = 10$ s

their demonstrated advantages but also their disadvantages and these have been discussed.

It has been demonstrated that TR reduction is generally without complications. The variation of flip angles, on the other hand, has a strong influence on the PSF and the resolution. The deleterious effects, a T_1 weighting of k-space, of this technique have been noted.

References

[1] T. Knubovets, H. Shinar, U. Eliav, G. Navon, A23Na multiple-quantum-filtered NMR study of the effect of the cytoskeleton conformation on the anisotropic motion of sodium ions in red blood cells, J. Magn. Reson. B 110 (1) (1996) 16–25.
[2] A. Pohlmeier, A. Oros-Peusquens, M. Javaux, M.I. Menzel, J. Vanderborght, J. Kaffanke, S. Romanzetti, J. Lindenmair, H. Vereecken, N.J. Shah, Changes in soil water content resulting from ricinus root uptake monitored by magnetic resonance imaging, Vadose Zone J. 7 (3) (2008) 1010–1017.
[3] B.J. Balcom, R.P. Macgregor, S.D. Beyea, D.P. Green, R.L. Armstrong, T.W. Bremner, Single-point ramped imaging with T1 enhancement (SPRITE), J. Magn. Reson. A 123 (1) (1996) 131–134.
[4] M. Halse, J. Rioux, S. Romanzetti, J. Kaffanke, B. MacMillan, I. Mastikhin, N.I. Shah, E. Aubanel, B.J. Balcom, Centric scan SPRITE magnetic resonance imaging: optimization of SNR, resolution, and relaxation time mapping, J. Magn. Reson. 169 (1) (2004) 102–117.

[5] M. Halse, D.J. Goodyear, B. MacMillan, P. Szomolanyi, D. Matheson, B.J. Balcom, Centric scan SPRITE magnetic resonance imaging, J. Magn. Reson. 165 (2) (2003) 219–229.
[6] A.A. Khrapitchev, B. Newling, B.J. Balcom, Sectoral sampling in centric-scan SPRITE magnetic resonance imaging, J. Magn. Reson. 178 (2) (2006) 288–296.
[7] P.J. Prado, B.J. Balcom, S.D. Beyea, R.L. Armstrong, T.W. Bremner, Concrete thawing studied by single-point ramped imaging, Solid State Nucl. Magn. Reson. 10 (1–2) (1997) 1–8.
[8] P.J. Prado, B.J. Balcom, I.V. Mastikhin, A.R. Cross, R.L. Armstrong, A. Logan, Magnetic resonance imaging of gases: A single-point ramped imaging with T1 enhancement (SPRITE) study, J. Magn. Reson. 137 (2) (1999) 324–332.
[9] C.B. Kennedy, B.J. Balcom, I.V. Mastikhin, Three dimensional magnetic resonance imaging of rigid polymeric materials using single point ramped imaging with T1 enhancement (SPRITE), Can. J. Chem. 76 (1998) 1753–1765.
[10] S. Romanzetti, M. Halse, J. Kaffanke, K. Zilles, B.J. Balcom, N.J. Shah, A comparison of three SPRITE techniques for the quantitative 3D imaging of the 23Na spin density on a 4T whole-body machine, J. Magn. Reson. 179 (1) (2006) 64–72.
[11] E.M. Haacke, R.W. Brown, M.R. Thompson, R. Venkatesan, Magnetic resonance imaging: physical principles and sequence design, Wiley, 1999.
[12] S. Gravina, D.G. Cory, Sensitivity and resolution of constant-time imaging, J. Magn. Reson. B 104 (1) (1994) 53–61.
[13] F.E. Boada, J.D. Christensen, F.R. Huang-Hellinger, T.G. Reese, K.R. Thulborn, Quantitative in vivo tissue sodium concentration maps: the effects of biexponential relaxation, Magn. Reson. Med. 32 (2) (1994) 219–223.
[14] C.J. Bergin, J.M. Pauly, A. Macovski, Lung parenchyma: projection reconstruction MR imaging, Radiology 179 (3) (1991) 777–781.
[15] I.V. Mastikhin, B.J. Balcom, P.J. Prado, C.B. Kennedy, SPRITE MRI with prepared magnetization and centric k-space sampling, J. Magn. Reson. 136 (2) (1999) 159–168.
[16] M.D. Robson, P.D. Gatehouse, M. Bydder, G.M. Bydder, Magnetic resonance: an introduction to ultrashort TE (UTE) imaging, J. Comput. Assist. Tomogr. 27 (6) (2003) 825–846.
[17] J.B. Kaffanke, T. Stöcker, S. Romanzetti, T. Dierkes, M.O. Leach, N.J. Shah, Phase-cycled averaging for the suppression of residual magnetisation in SPI sequences, J. Magn. Reson., in press, doi:10.1016/j.jmr.2008.11.018.